Spectral statistics of a pseudo-integrable map: the general case

2009 Nonlinearity 22 2101

(http://iopscience.iop.org/0951-7715/22/9/003)

IOP PUBLISHING NONLINEARITY

Nonlinearity **22** (2009) 2101–2126 doi:10.1088/0951-7715/22/9/003

Spectral statistics of a pseudo-integrable map: the general case*

E Bogomolny[1], **R Dubertrand**[1,2] **and C Schmit**[1]

[1] Université Paris-Sud, CNRS, UMR 8626, Laboratoire de Physique Théorique et Modelès Statistiques, 91405 Orsay Cedex, France
[2] Department of Mathematics, University of Bristol, BS8 1TW, UK

Received 13 March 2009, in final form 28 May 2009
Published 21 July 2009
Online at stacks.iop.org/Non/22/2101

Recommended by L Bunimovich

Abstract
It is well established numerically that spectral statistics of pseudo-integrable models differs considerably from the reference statistics of integrable and chaotic systems. In Bogomolny and Schmit (2004 *Phys. Rev. Lett.* **93** 254102) statistical properties of a certain quantized pseudo-integrable map had been calculated analytically but only for a special sequence of matrix dimensions. The purpose of this paper is to obtain the spectral statistics of the same quantum map for all matrix dimensions.

Mathematics Subject Classification: 37E10, 15A52, 81Q10, 81Q50

(Some figures in this article are in colour only in the electronic version)

1. Introduction

The relation between spectral statistics of a quantum system and its classical counterpart is one of the main achievements of quantum chaos. It is established that at the scale of the mean level density the spectral statistics of classically integrable systems are described by the Poisson distribution [1] and the spectral statistics of classically chaotic systems are close to the statistics of eigenvalues of standard random matrix ensembles depending only on the underlying symmetry [2]. Though these statements had not mathematically been proved in the full generality and there exist noticeable exceptions (e.g. chaotic systems on constant negative curvature surfaces generated by arithmetic groups [3]), these conjectures are widely accepted for 'generic' quantum systems.

Much less is known when a system is not classically integrable or completely chaotic. An important example which we have in mind is the case of pseudo-integrable systems (see e.g. [4]) represented by two-dimensional polygonal billiards whose each angle is a rational

* This article is dedicated to the memory of Charles Schmit.

multiple of π. A typical classical trajectory in such models covers a two-dimensional surface of a finite genus $\geqslant 2$ [5]. For comparison, a trajectory of a two-dimensional integrable model belongs to a two-dimensional torus of genus 1 and a typical trajectory of a two-dimensional chaotic system covers ergodically the whole three-dimensional surface of constant energy.

Numerical calculations [6] clearly demonstrated that the spectral statistics of pseudo-integrable billiards is not universal and depends on billiard angles. It appears that the spectral statistics of such models has two characteristic features: a level repulsion at small distances and an exponential decrease in the nearest-neighbour distribution at large separations. This type of statistics (called intermediate statistics) has been observed for the first time in the numerical simulations of the Anderson model at the point of metal–insulator transition [7] and later in this context has been profoundly investigated (see e.g. a recent review [8] and references therein). Unfortunately analytical progress in the investigation of intermediate statistics in pseudo-integrable systems is limited. In [9] the level compressibility of certain pseudo-integrable billiards was computed analytically, thus confirming the intermediate character of their spectral statistics. The main difficulty in the analytical treatment of two-dimensional pseudo-integrable billiards is the strong diffraction on billiard corners with angles $\neq \pi/n$ with integer n. Though there exists the exact Sommerfeld's solution for the scattering on such angles [10], the diffraction coefficient is formally infinite along the optical boundaries so it is impossible to treat the multiple corner diffraction in perturbation series. A certain progress has been made in [11] where it was found that the multiple diffraction along periodic orbit channels in pseudo-integrable systems forces the wave functions to tend to zero on the channel boundaries thus forming superscarring states observed recently in micro-wave experiments [12].

The difficulties in analytical solution of pseudo-integrable billiards lead to the necessity of investigation of simpler models with similar features. A promising example is the quantization of interval exchange maps which are known to be the correct description of classical dynamics in pseudo-integrable systems [4, 5].

In [13] the following classical parabolic map had been quantized:

$$\Phi_\alpha : \begin{pmatrix} p \\ x \end{pmatrix} \Longrightarrow \begin{pmatrix} p+\alpha \\ x+f(p+\alpha) \end{pmatrix} \bmod 1. \tag{1}$$

Here α is a constant and $f(p)$ is a certain function (taken equal to $2p$ in [13]). For rational $\alpha = m/q$ this map corresponds to the simplest interval exchange map of two intervals.

After a straightforward generalization of the results of [13] the $N \times N$ unitary matrix associated with the above map has the form of the diagonal matrix $\mathrm{e}^{\mathrm{i}\Phi_k}$ with real Φ_k multiplied by a constant unitary matrix μ_{kp} ($k, p = 0, 1, \ldots, N-1$):

$$M_{kp} = \mathrm{e}^{\mathrm{i}\Phi_k}\mu_{kp}\ , \tag{2}$$

where $\Phi_k = -2\pi N F(k/N)$ with $F'(p) = f(p)$ and

$$\mu_{kp} = \frac{1}{N}\sum_{r=0}^{N-1} \exp\left[\frac{2\pi \mathrm{i}}{N} r(k-p+\alpha N)\right] = \frac{1-\mathrm{e}^{2\pi \mathrm{i}\alpha N}}{N(1-\mathrm{e}^{2\pi \mathrm{i}(k-p+\alpha N)/N})}\ . \tag{3}$$

The matrix μ_{kp} depends on a parameter α and the last equality is valid when αN is not an integer. (In the latter case the spectrum of (2) can be obtained analytically [14] and we always assume below that for rational $\alpha = m/q, mN \not\equiv 0 \bmod q$.)

Because Φ_k in (2) are defined modulo 2π many increasing functions $F(p)$ will effectively correspond to pseudo-random phases distributed between 0 and 2π. As it was done in [15] we consider two typical cases. The first corresponds to the ensemble of random matrices (2) where all N phases Φ_k are considered as independent random variables distributed uniformly

between 0 and 2π. We call such matrices non-symmetric ensemble. In the second case only a half of the phases are independent random variables uniformly distributed between 0 and 2π. The other half is related to the first one by the symmetry

$$\Phi_{N-k} = \Phi_k, \qquad k = 1, \ldots, \left[\frac{N}{2}\right]. \tag{4}$$

This case will be called the symmetric ensemble as in the dynamical interpretation the transformation $k \to -k$ is the time-inversion symmetry.

The eigenvalues Λ_n and the eigenvectors $u_k(n)$, $n = 1, 2, \ldots, N$, are defined as usual

$$\Lambda_n u_k(n) = \sum_{p=0}^{N-1} M_{kp} u_p(n) \ . \tag{5}$$

Because matrix M_{kp} is unitary ($M\,M^{\dagger} = 1$), its eigenvalues lie on the unit circle

$$\Lambda_n = \mathrm{e}^{\mathrm{i}\theta_n} \tag{6}$$

and its eigenvectors can be chosen orthonormal

$$\sum_{k=0}^{N-1} \bar{u}_k(m) u_k(n) = \delta_{mn}. \tag{7}$$

The statistical properties of matrix (2) depend crucially on the arithmetic of the parameter α. For irrational α the map (1) is only a parabolic map and methods developed in [15] and in this paper cannot be directly applied. Numerical calculations suggest that for Diophantine α the spectral statistics of the matrix (2) is very close to the standard statistics of the Gaussian ensembles of random matrices [16]. Namely, non-symmetric matrices are described by the GUE statistics and symmetric matrices by the GOE statistics. For illustration in figure 1 we plot the nearest-neighbour distribution for matrices (2) with $\alpha = \sqrt{5}/4$ and $N = 801$. The solid lines indicates the Wigner surmise (8) which is known (see e.g. [16]) to be a good approximation for the GUE and the GOE distributions.

$$p_{\mathrm{GUE}}(s) = \frac{32}{\pi^2} s^2 \mathrm{e}^{-4s^2/\pi}, \qquad p_{\mathrm{GOE}}(s) = \frac{\pi}{2} s \mathrm{e}^{-\pi s^2/4}. \tag{8}$$

Rational $\alpha = m/q$ with co-prime integers m and q correspond to an interval exchange map [13] and we shall consider only such values of α throughout the paper.

This paper investigates the following question: What are the statistical properties of eigenvalues of the matrix (2) for fixed rational $\alpha = m/q$ and large N? It appears that to get a well-defined limit in this case it is necessary to consider increasing sequences of matrix dimensions, N, such that the product of the numerator of α times N has a fixed residue modulo the denominator of α

$$mN \equiv k \bmod q. \tag{9}$$

In [15] it was demonstrated that for a special sequence of matrix dimensions with

$$mN \equiv \pm 1 \bmod q \tag{10}$$

eigenvalues of the matrices (2) and (3) are described by the so-called semi-Poisson statistics which has been proposed in [17] as the simplest model of intermediate statistics.

Let $x_1 \leqslant x_2 \leqslant \ldots \leqslant x_K$ be an ordered sequence of real numbers (eigenvalues). The joint distribution for the semi-Poisson statistics is proportional to the product of the nearest distances between these level times a confining potential $V(x)$:

$$P(x_1, x_2, \ldots, x_K) \sim \prod_i |x_{i+1} - x_i|^{\beta} \prod_i .\mathrm{e}^{-V(x_i)}. \tag{11}$$

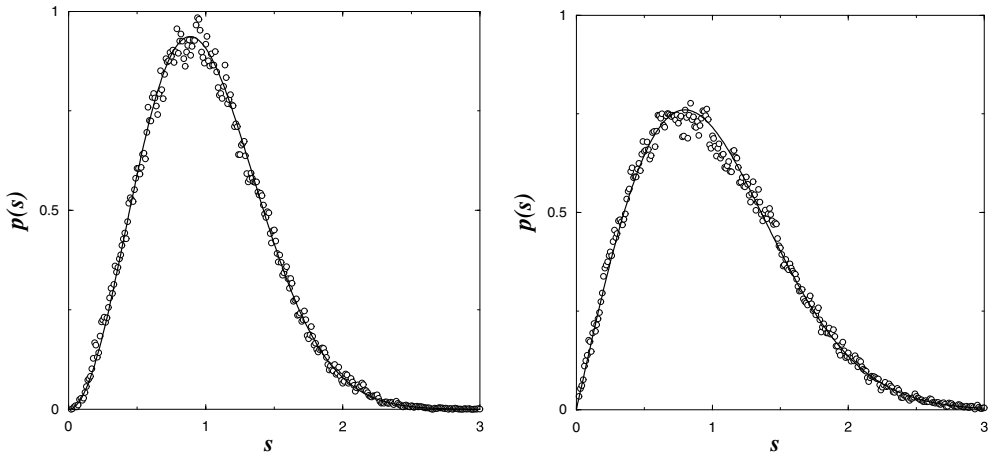

Figure 1. Open circles are nearest-neighbour distribution with $\alpha = \sqrt{5}/4$ and $N = 801$ for non-symmetric matrices (a) and symmetric matrices (b). Solid lines indicate the Wigner surmise (8).

In the limit $K \to \infty$ all correlation functions of the semi-Poisson statistics at the scale of the mean level density do not depend on $V(x)$ and can be obtained analytically [17]. In particular, the probability that between two levels there exist exactly $n-1$ levels has the form

$$p_n(\beta; s) = \frac{(\beta+1)^{n\beta+n}}{\Gamma(n\beta+n)} s^{n\beta+n-1} \mathrm{e}^{-(\beta+1)s}. \tag{12}$$

The semi-Poisson statistics depends only on one parameter β which fixes the level repulsion at small distances so the nearest-neighbour distribution (i.e. $p_n(\beta; s)$ for $n = 1$) tends to zero as s^β:

$$p(\beta; s) = A_\beta s^\beta \mathrm{e}^{-(\beta+1)s} \tag{13}$$

with $A_\beta = (\beta+1)^{\beta+1}/\Gamma(\beta+1)$.

From a mathematical point of view the semi-Poisson statistics can be considered as a stochastic process with independent increments (with gamma distribution) forming a convolution semigroup

$$(p_n * p_m)(\beta; s) \equiv \int_0^s p_n(\beta; y) p_m(\beta; s-y)\, \mathrm{d}y = p_{n+m}(\beta; s). \tag{14}$$

According to [15] when the condition (10) is satisfied the spectral statistics of the matrix (2) tends for large N to the semi-Poisson distribution with the following integer and half integer values of β depending on the denominator of $\alpha = m/q$ and the symmetry of the map:

$$\beta = \begin{cases} q-1 & \text{for non-symmetric ensemble} \\ \frac{1}{2}q - 1 & \text{for symmetric ensemble} \end{cases}. \tag{15}$$

To compare numerical calculations with theoretical predictions it is often more precise to consider instead of the nearest-neighbour distribution, $p(s)$, (as in figure 1) its integral

$$N(s) \equiv \int_0^s p(s')\, \mathrm{d}s' \tag{16}$$

which gives the relative number of levels when the distance between the nearest-neighbour eigenvalues is less than s.

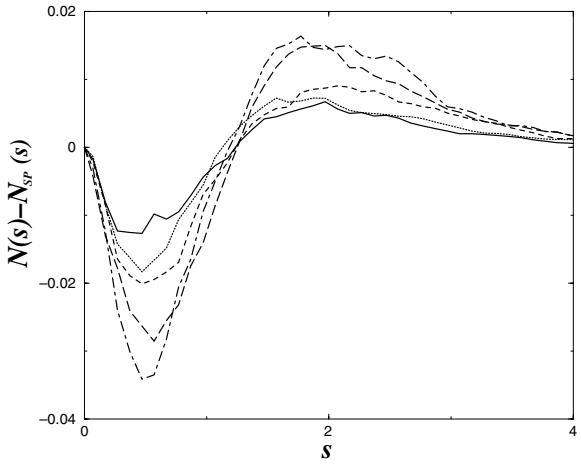

Figure 2. Differences between the integrated nearest-neighbour distributions for the non-symmetric ensemble of matrix (2) with $\alpha = 1/2$ for different odd N and the theoretical prediction for this case (17). The different lines from bottom to top at small s correspond, respectively, to $N = 101$, 201, 401, 801 and 1601.

To illustrate the convergence of the spectral statistics of the above matrices to the predicted values let us consider e.g. $\alpha = 1/2$ with odd N. From (15) and (13) it follows that the limiting integrated nearest-neighbour distribution in the non-symmetric case is here the simplest semi-Poisson distribution with $\beta = 1$:

$$N_{\rm sp} = 1 - (2s + 1)\mathrm{e}^{-2s}. \tag{17}$$

In figure 2 the difference between the integrated nearest-neighbour distribution computed numerically and its theoretical prediction (17) is plotted for different odd matrix dimensions. For this and other similar figures in the paper the number of realizations is chosen to be the minimum between 100 and $50\,000/N$. The figure shows that the agreement is quite good (less than 0.02) even for N of the order of a few hundreds.

The purpose of this paper is to calculate the spectral statistics of the above quantized pseudo-integrable map in the general case (9) with $k \neq 0, \pm 1 \bmod q$. The plan of the paper is the following. Sections 2 and 3 give extended details of the construction briefly discussed in [15]. The peculiarity of the problem under consideration is the existence of 2 rank-one deformations of the original matrix (2) with known eigenvalues and eigenvectors. These deformations are discussed in section 2. In section 3 it is demonstrated that these rank-one deformations lead to long-range correlations between the eigenvalues of the initial matrix (2). To obtain a clear picture of these correlations it is convenient to use a special form of eigenvalue ordering (an analogue of the unfolding) which is discussed in section 4. In section 5 it is shown that these long-range correlations can effectively be taken into account by the construction of a kind of transfer operator. This operator is a finite dimensional matrix whose largest eigenvalue and corresponding eigenvectors permit to calculate all correlation functions. This is done explicitly for a few main examples in section 6. Obtained analytical formulae agree well with numerical calculations. The summary of the results is present in section 7. Certain technical details are given in the appendices.

2. Rank-one deformations

As was shown in [15] the important property of the matrices (2) and (3) is the possibility to rewrite it in the following form

$$M_{kp} \equiv \mathrm{e}^{\mathrm{i}\Phi_k} \frac{(1-\mathrm{e}^{2\pi\mathrm{i}\alpha N})}{N(1-\mathrm{e}^{2\pi\mathrm{i}(k-p+\alpha N)/N})} = N_{kp} + \frac{1-\mathrm{e}^{2\pi\mathrm{i}\alpha N}}{N}\mathrm{e}^{\mathrm{i}\Phi_k} \tag{18}$$

where a new matrix N_{kp} is

$$N_{kp} = M_{kp}\mathrm{e}^{2\pi\mathrm{i}(k-p+\alpha N)/N}\,. \tag{19}$$

Eigenvalues Λ'_n and eigenvectors $\psi_k(n)$ of the matrix N_{kp},

$$\Lambda'_n\psi_k(n) = \sum_{p=0}^{N-1} N_{kp}\psi_p(n), \tag{20}$$

can easily be expressed through the eigenvalues and the eigenvectors of the original matrix M_{kp},

$$\psi_k(n) = \mathrm{e}^{2\pi\mathrm{i}k/N}u_k(n), \qquad \Lambda'_n = \mathrm{e}^{2\pi\mathrm{i}\alpha}\Lambda_n. \tag{21}$$

But from (18) it follows that matrix N_{kp} is a rank-one deformation of matrix M_{kp} so it is possible to construct its eigenvalues and the corresponding eigenvectors in a different way (see e.g. [18]).

Write a formal expansion of an eigenvector of matrix N_{kp} as a series of the complete set of eigenvectors of the matrix M_{kp}:

$$\psi_k(n) \equiv \mathrm{e}^{2\pi\mathrm{i}k/N}u_k(n) = \sum_{m=1}^{N} c_m(n)u_k(m). \tag{22}$$

From (18) one gets

$$\Lambda'_n\sum_{m=1}^{N} c_m(n)u_k(m) = \sum_{m=1}^{N} c_m(n)\Lambda_m u_k(m) - \frac{1-\mathrm{e}^{2\pi\mathrm{i}\alpha N}}{N}\mathrm{e}^{\mathrm{i}\Phi_k}\sum_{m=1}^{N} c_m(n)\sum_{p=0}^{N-1} u_p(m). \tag{23}$$

Introducing the notations

$$A_m = \sum_{k=0}^{N-1} u_k(m), \qquad g(n) = \sum_{m=1}^{N} c_m(n)A_m \tag{24}$$

and using the orthogonality of eigenvectors $u_k(n)$ (7) one obtains

$$c_m(n) = \frac{1-\mathrm{e}^{2\pi\mathrm{i}\alpha N}}{N}g(n)\frac{B_m}{\Lambda_m - \Lambda'_n}, \tag{25}$$

where

$$B_m = \sum_{k=0}^{N-1}\mathrm{e}^{\mathrm{i}\Phi_k}\bar{u}_k(m). \tag{26}$$

Multiplying both sides of (25) by A_m and summing from 1 to N one concludes that every eigenvalues Λ'_m of the matrix N_{kp} obey the equation

$$1 = \frac{1-\mathrm{e}^{2\pi\mathrm{i}\alpha N}}{N}\sum_{m=1}^{N}\frac{A_m B_m}{\Lambda_m - \Lambda'_n}. \tag{27}$$

From (5) and (3) it follows that

$$\Lambda_m\bar{B}_m = A_m \tag{28}$$

and equation (27) takes the final form

$$1 = \frac{1 - \mathrm{e}^{2\pi \mathrm{i}\alpha N}}{N} \sum_m \frac{\Lambda_m |B_m|^2}{\Lambda_m - \Lambda'_n}. \tag{29}$$

For rank-one deformations of a real symmetric matrix all terms in the corresponding equation would be real and one easily comes to the well-known conclusion that the eigenvalues of a rank-one deformation of a real symmetric matrix are in-between the eigenvalues of the unperturbed ones (cf [18]). In our case both the matrices, M_{kp} and N_{kp}, are unitary and their eigenvalues lie on the unit circle: $\Lambda_m = \mathrm{e}^{\mathrm{i}\theta_m}$, $\Lambda'_n = \mathrm{e}^{\mathrm{i}\theta'_n}$. So arguments require straightforward modifications.

From (29) one gets

$$\frac{N}{1 - \mathrm{e}^{2\pi \mathrm{i}\alpha N}} = \sum_m \frac{|B_m|^2}{1 - \mathrm{e}^{\mathrm{i}(\theta'_n - \theta_m)}}, \tag{30}$$

which can be rewritten as follows:

$$N(\cot \pi\alpha N - \mathrm{i}) = \sum_m |B_m|^2 \left(\cot \frac{\theta'_n - \theta_m}{2} - \mathrm{i} \right). \tag{31}$$

Due to the completeness of $u_k(m)$ one has

$$\sum_{n=1}^{N} \bar{u}_p(n) u_k(n) = \delta_{pk}. \tag{32}$$

and, consequently,

$$\sum_{m=1}^{N} |B_m|^2 = N. \tag{33}$$

Therefore, the imaginary part of (31) is identically zero and new phases θ'_n have to be determined from a real equation

$$F(\theta'_n) = N \cot \pi\alpha N, \tag{34}$$

where $F(\theta)$ is defined by

$$F(\theta) = \sum_{m=1}^{N} |B_m|^2 \cot \frac{\theta - \theta_m}{2}. \tag{35}$$

In the interval $[0, 2\pi)$ $F(\theta)$ has poles at $\theta = \theta_m$ (assuming that all $B_m \neq 0$) and it is monotone between them (cf figure 3). Let the eigenphases θ_m be ordered on the unit circle $0 \leqslant \theta_1 \leqslant \theta_2 \leqslant \ldots \leqslant \theta_N < 2\pi$. Then between two nearby eigenvalues θ_m and θ_{m+1} $(\mathrm{mod}\, 2\pi)$ there exists one and only one new eigenvalue θ'_n. Here the new eigenvalues are not necessarily ordered. But according to (21) all eigenphases of the matrix N_{kp} have the form $\theta'_m = \theta_m + 2\pi\alpha$ $(\mathrm{mod}\, 2\pi)$. Therefore we prove the following lemma (cf figure 4).

Lemma 1. *The eigenvalues of the unitary matrix M_{kp} defined in (2) and (3) are such that after the rotation by $2\pi\alpha$ in-between any pairs of nearest eigenvalues there exists one and only one rotated eigenvalue.*

Multiplying (18) by $\exp(-2\pi \mathrm{i}(k - p + \alpha N)/N)$ one gets another relation

$$M_{kp} = \tilde{N}_{kp} - \frac{1 - \mathrm{e}^{2\pi \mathrm{i}\alpha N}}{N} \mathrm{e}^{\mathrm{i}\Phi_k - 2\pi \mathrm{i}(k - p + \alpha N)/N} \tag{36}$$

with a new matrix $\tilde{N}_{kp}$

$$\tilde{N}_{kp} = M_{kp} \mathrm{e}^{-2\pi \mathrm{i}(k - p + \alpha N)/N} \tag{37}$$

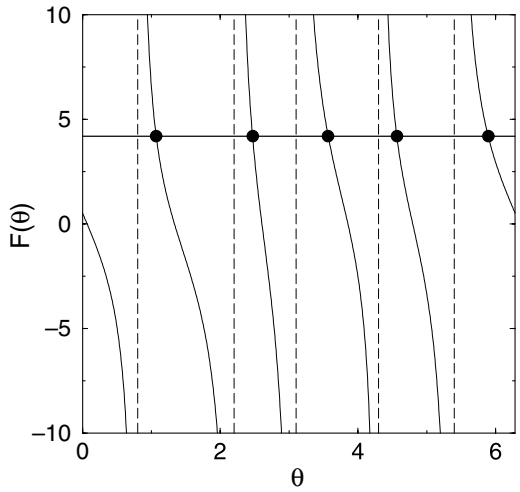

Figure 3. Schematic plot of equation (34) (solid black line). $F(\theta)$ is defined by (35). Vertical dashed lines represent the pole positions. Horizontal straight line indicates the value of the right-hand side of equation (34). The abscissa of its intersections with $F(\theta)$ (indicated by black circles) give the solutions of that equation.

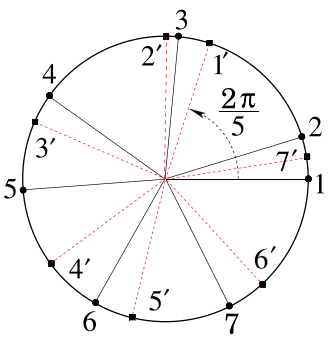

Figure 4. Illustration of lemma 1. Black circles denote the position of 7 eigenphases for $\alpha = 1/5$ and black lines are their radius vectors. Black squares indicate the position of eigenphases after the rotation by angle $2\pi/5$ and the dashed red lines are radius vectors of the rotated eigenphases. The rotated points are indicated by the same number but with sign′.

whose eigenvalues and eigenvectors are

$$\tilde{\psi}_k(n) = \mathrm{e}^{-2\pi \mathrm{i}k/N} u_k(n), \qquad \tilde{\Lambda}'_n = \mathrm{e}^{-2\pi \mathrm{i}\alpha} \Lambda_n. \tag{38}$$

Repeating the above calculations but for the matrix $\tilde{N}_{kp}$ one finds that its eigenvalues $\tilde{\Lambda}'_m$ have to be determined from the equation

$$1 = \frac{1 - \mathrm{e}^{2\pi \mathrm{i}\alpha N}}{N} \sum_{m=1}^{N} \frac{\Lambda_m |\tilde{B}_m|^2}{\Lambda_m - \tilde{\Lambda}'_n}, \tag{39}$$

where

$$\tilde{B}_m = \sum_{k=0}^{N-1} \bar{u}_k(m) \mathrm{e}^{\mathrm{i}\Phi_k - 2\pi \mathrm{i}k/N}. \tag{40}$$

As it has exactly the same form as (29) and $\tilde{\Lambda}'_n = \mathrm{e}^{-2\pi \mathrm{i}\alpha} \Lambda_n$ one comes to the lemma.

Lemma 1′. *The eigenvalues of M_{kp} are such that after the rotation by $-2\pi\alpha$ between two nearest eigenvalues of M_{kp} there exists one and only one rotated eigenvalue.*

These lemmas prove the existence of long-range correlations between eigenvalues of the matrix M_{kp} which are merely a consequence of the fact that rank-one deformations (18) and (36) of the original matrix (2) have eigenvalues easily expressible through eigenvalues of the original matrix.

A few other consequences of this property is worth mentioning. As all N solutions of (29) have the form $\Lambda'_n = \Lambda_n e^{2\pi i\alpha}$ with $n = 1, \ldots, N$ the numerators of this equation can be found explicitly. From appendix A it follows that

$$\frac{1 - e^{2\pi i\alpha N}}{N} \Lambda_m |B_m|^2 = \frac{\prod_{n=1}^{N} (\Lambda_m - \Lambda_n e^{2\pi i\alpha})}{\prod_{s\neq m} (\Lambda_m - \Lambda_s)}, \tag{41}$$

which can be rewritten in the real form as follows

$$|B_m|^2 \frac{\sin \pi\alpha N}{N \sin \pi\alpha} = \prod_{n\neq m} \frac{\sin(\frac{1}{2}(\theta_m - \theta_n - 2\pi\alpha))}{\sin(\frac{1}{2}(\theta_m - \theta_n))}. \tag{42}$$

Similarly, from (39) one concludes that

$$\frac{1 - e^{-2\pi i\alpha N}}{N} \Lambda_m |\tilde{B}_m|^2 = \frac{\prod_{n=1}^{N} (\Lambda_m - \Lambda_n e^{-2\pi i\alpha})}{\prod_{s\neq m} (\Lambda_m - \Lambda_s)}. \tag{43}$$

So

$$|\tilde{B}_m|^2 \frac{\sin \pi\alpha N}{N \sin \pi\alpha} = \prod_{n\neq m} \frac{\sin(\frac{1}{2}(\theta_m - \theta_n + 2\pi\alpha))}{\sin(\frac{1}{2}(\theta_m - \theta_n))}. \tag{44}$$

3. Long-range correlations

In the preceding sections it has been proved that eigenphases of matrix (5) have a special type of long-range correlations. Namely, when one rotates all eigenvalues of this matrix by $\pm 2\pi\alpha$ and superimposes the rotated eigenphases with non-rotated ones then in-between two nearest eigenvalues of the original matrix there will be one and only one rotated eigenphase. In this section we investigate certain consequences of such correlations in more details.

Let us put all eigenvalues of unitary matrix (2) on the unit circle and consider a sector of angle $2\pi\alpha$ which contains n eigenvalues (see figure 5(a)). The sector boundaries divide the unit circle in-between certain eigenphases. Denote the angular distance from the sector boundaries to the nearest eigenphases in the clockwise and counterclockwise directions by y_k, y_{k+1} and x_k, x_{k+1}, respectively (cf figure 5(a)). We choose by convention to take $y_k = 0$ if one eigenvalue lies exactly on the boundary of the sector. The reason for these notations will become clearer on the following page. After the rotation by $2\pi\alpha$ only two possibilities are possible: either the point x_k or the point y_k will fall inside the points x_{k+1} and y_{k+1}. In the first case one has $x_k < x_{k+1}$ and $y_{k+1} < y_k$. In the second case the inequalities are reversed: $x_k > x_{k+1}$ and $y_{k+1} > y_k$. Therefore in the all cases the following inequality is fulfilled:

$$(y_{k+1} - y_k)(x_{k+1} - x_k) < 0. \tag{45}$$

This inequality is valid for all α and N. From now on we shall consider only rational α:

$$\alpha = \frac{m}{q} \tag{46}$$

with co-prime integers m and q.

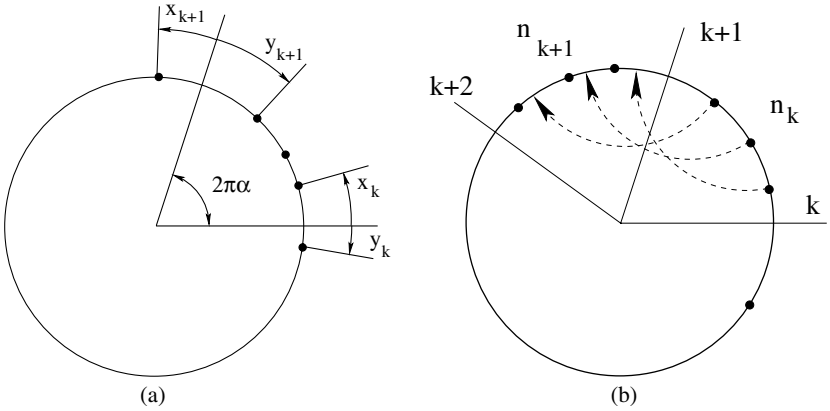

Figure 5. (*a*) Eigenphases close to the boundaries of a $2\pi\alpha$ sector. (*b*) Division of the unit circle into sectors of angle $2\pi m/q$. Black circles indicate the position of eigenphases in two nearby sectors. Dashed lines show the positions which will occupy eigenvalues from one sector after the rotation by $2\pi m/q$.

As above divide the unit circle into q radial sectors of angle $2\pi m/q$. When $m = 1$ these sectors are disjoint but for $m > 1$ they will overlap. Denote the number of eigenphases in the kth sector by n_k (see figure 5(*b*)).

After the rotation by $2\pi m/q$ the eigenphases from the kth sector will move into the $(k+1)$th sector. These rotated points will divide this sector into $n_k + 1$ intervals. According to lemma 1 the eigenphases in the $(k + 1)$th sector have to be intertwined with the rotated eigenvalues. Therefore, all intervals except the first and the last have to be occupied. The first will be occupied if $x_k > x_{k+1}$ and the last will be occupied if $y_{k+1} > y_{k+2}$. All these requirements can be rewritten as the following recurrence relation:

$$n_{k+1} = n_k - 1 + \Theta(x_k - x_{k+1}) + \Theta(y_{k+1} - y_{k+2})\ . \tag{47}$$

Here as in figure 5(*a*) x_k and y_k are distances from the boundary of the kth sector to the two closest eigenphases to it and $\Theta(x)$ is the Heaviside function: $\Theta(x) = 1$ if $x > 0$ and $\Theta(x) = 0$ if $x < 0$. From (45) it follows that the difference $y_{k+1} - y_{k+2}$ is of opposite sign from the difference $x_{k+1} - x_{k+2}$ and the last relation takes the form

$$n_{k+1} = n_k - 1 + \Theta(x_k - x_{k+1}) + \Theta(x_{k+2} - x_{k+1}). \tag{48}$$

Now choose the beginning of the first sector at the position of an eigenphase (i.e. impose $y_1 = 0$). Then from (45) it follows that $x_2 < x_1$ and $x_q < x_1$. Direct applications of (48) give

$$n_2 = n_1 - 1 + \Theta(x_1 - x_2) + \Theta(x_3 - x_2) = n_1 + \Theta(x_3 - x_2) \tag{49}$$

because $x_1 > x_2$,

$$\begin{aligned} n_3 &= n_2 - 1 + \Theta(x_2 - x_3) + \Theta(x_4 - x_3) \\ &= n_1 + \Theta(x_3 - x_2) - 1 + \Theta(x_2 - x_3) + \Theta(x_4 - x_3) = n_1 + \Theta(x_4 - x_3) \end{aligned} \tag{50}$$

because $\Theta(x) + \Theta(-x) = 1$ and so on. In this manner one concludes that for $j = 2, \ldots, q-1$

$$n_j = n_1 + \Theta(x_{j+1} - x_j) \tag{51}$$

and $n_q = n_1 + 1$ because, as was noted above, $x_q < x_1$.

As the sum over all q sectors cover the unit circle m times, the sum over all n_k equals mN: $\sum_{k=1}^{q} n_k = mN$. Therefore

$$mN = qn_1 + 1 + \sum_{j=2}^{q-1} \Theta(x_{j+1} - x_j). \tag{52}$$

When $mN \equiv 1 \bmod q$, all Θ-functions on the right-hand side of this expression are forced to be zero which leads to the conclusion that in this case

$$x_q < x_{q-1} < \ldots < x_2 < x_1. \tag{53}$$

When $mN \equiv -1 \bmod q$, all Θ-functions have to be equal to 1 and the inequalities are reversed

$$x_2 < x_3 < \ldots < x_{q-1} < x_q < x_1. \tag{54}$$

Inequalities (53) and (54) manifest the existence of an exceptionally strong long-range correlations when $mN \equiv \pm 1 \bmod q$. For usual matrix ensembles correlations between eigenvalues separated by a large distance tend to zero. But in our case eigenphases at distances $2\pi mk/q$ with $k = 1, \ldots, (q-1)$ are not independent but restricted by the above inequalities. In [15] only these special cases had been considered.

4. Geometrical unfolding

Inequalities (45) and recurrence relations (48) include eigenvalues separated by distances of the order of $2\pi/q$ where q is the denominator of α. On the other hand, the mean level density equals $2\pi/N$ where N is the matrix dimension. As we are interested in the case $N \to \infty$ with q fixed, the restrictions implied by (45) and (48) are of long range which makes it difficult to incorporate them for calculations of correlation functions of nearby levels. In this section we show that these long-range restrictions can be transformed by geometrical unfolding into a more tractable form.

Let us split the unit circle into q angular sectors of angle $2\pi m/q$ as above and denote the positions of eigenvalues inside each sector on q horizontal lines numerated from bottom to top by numbers from 1 to q (see figure 6). As the last and the first sectors are connected, it is useful to draw vertical lines from points at the lowest horizontal line (i.e. eigenvalue positions inside the first sector) till they cross the highest horizontal line. In such a way this last line will contain two sets of points. The first indicates eigenvalue positions inside the last sector and the second reports the images of the first sector points after the rotation by $-2\pi m/q$. From the condition $x_q < x_1$ proved in the previous section it follows that these two groups of points intertwine and at the qth line between two nearby vertical lines there is one and only one eigenvalue point.

Below we shall construct different staircase lines. Each starts from a point on the lowest horizontal line, goes right and up, and ends on the last horizontal line at the image of another lowest line point. The distance along the lowest line between the final and the initial points is divided by consecutive eigenvalues into a certain number of intervals. If this number equals k we will say that the staircase line has the shift (or shifted) by k units.

According to lemmas 1 and 1′, between two closest eigenphases of the matrix (2) there is one and only one eigenphase rotated by $2\pi\alpha = 2\pi m/q$. In the unfolded description it is manifested by the condition that points at each line have to be in-between two close-by points on the lower line. The relative positions of eigenvalues strongly depend on distances x_k from the beginning of each sector to the eigenphase closest to it (see (52)). In the unfolded representation (as in figure 6(*a*)) x_k are the distances along the horizontal lines to points closest to a vertical line which represents the boundary of a sector with angle $2\pi m/q$.

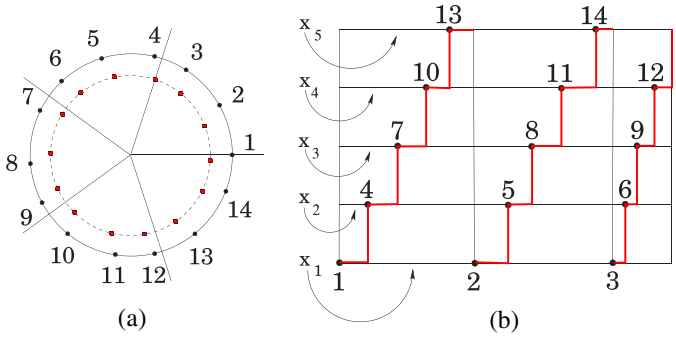

Figure 6. (*a*) Small black circles: schematic view of eigenvalues of matrix (2) for $\alpha = 1/5$ and $N = 14$ ($N \equiv -1 \bmod 5$). Numbers from 1 to 14 indicate the consecutive eigenphases. Eigenphases rotated by $2\pi/5$ are denoted by red squares. For clarity they are situated on a smaller dashed circle. (*b*) The same configuration of eigenvalues but unfolded on five horizontal lines representing 5 sectors. $x_1, \ldots, x_5$ are the distances from the beginning of the sectors to the closest eigenphase as in figure 5(*a*), thick red lines demonstrate relative eigenvalue positions.

Let us start from the lower left point and draw a horizontal line till there is at the vertical a point situated at the first line above it. Then draw the vertical line till it touches that point. Now continue drawing a horizontal line till there is at the vertical a point at the upper line closest to the boundary of the given sector and so on. This line will go right if $x_{k+1} > x_k$ and left if $x_{k+1} < x_k$. Finally, points will be connected by stepwise lines as in figure 6(*b*). Note that according to our convention point 1 does not belong to the first line but to the last one. The shape of these lines are determined by the inequalities between all x_k. In figure 6 the case of $N \equiv -1 \bmod 5$ is indicated. According to (54) $x_{k+1} > x_k$ for $k = 1, \ldots, 4$ which explains the staircase form of these lines. They all start at points along the first horizontal line, go up and to the right, and finally finish at the last horizontal line but with the shift by 1 unit. It is clear that such lines cannot cross each other.

For other matrix dimensions these lines will have a different shape. Consider first as an example the case $\alpha = 1/5$ and $N \equiv -2 \bmod 5$. From (52) it follows that in this case only 2 of 3 Θ-functions have to be equal to 1. Every time one of the Θ-functions is zero, the above lines turn to the left (see figure 7) so the shape of the stepwise curve differs from the one of figure 6(*b*). Consider the horizontal line when it first turns left. Instead of the left turn let us continue to the right till we touch another point on this line. As between these two points there exists only one point at the lower and higher lines there is no contradiction with our line construction (cf figure 7). Finally we come to the conclusion that for these values of α and N the eigenphases have to be connected by non-intersecting lines which go only up and to the right and whose initial and final points are shifted by 2 units.

These arguments can be generalized for all values of matrix dimensions and we get the following description of the local unfolded structure of the eigenvalues:

Claim. *For $\alpha = m/q$ and $mN \equiv -k \bmod q$, the mutual positions of eigenphases of matrix (2) can be described as follows. Fix q horizontal lines, put arbitrary points at the lowest line, and note the vertical images of these points along the last line. Draw staircase non-intersecting lines going only up and to the right with the condition that they start at the lower line and end at last line but with the shift by k units. Points at horizontal lines are situated at the corners of the constructed lines.*

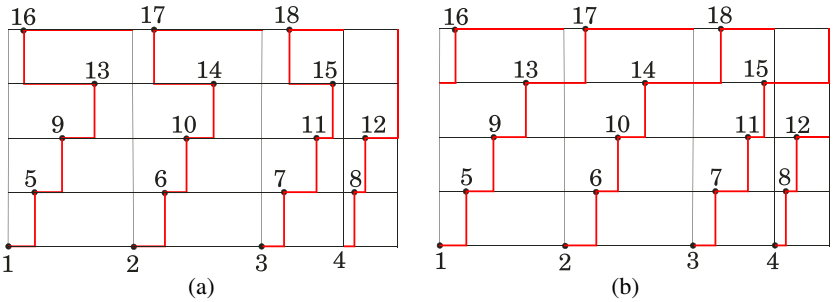

Figure 7. (*a*) Small black circles: schematic view of the eigenvalues of matrix (2) for $\alpha = 1/5$ and $N = 18$ (i.e. $N \equiv -2 \bmod 5$). The thick red lines connect eigenphases as indicated in the text. (*b*) The same configuration of eigenvalues but connected by non-decreasing staircase lines.

Proof. Start from the lowest left point and draw the staircase line using the same rules as above but this time we will always go right along the horizontal lines. When this staircase line touches the last qth horizontal line we will continue it right till the closest vertical line, and then we stop the process. From lemma 1 it follows that the first vertical segment cannot be shifted more than 1 unit (i.e. it cannot cross vertical line emanating from the first point along the lowest horizontal line closest from the right to the initial point). The second vertical segment of the constructed staircase line cannot be shifted more than 2 units and so on. Finally the full staircase line will have a certain shift between 1 unit and $q - 1$ units.

Now repeat the construction of the staircase line but starting from the closest point to the right of the first point (cf figure 7(*b*)). By construction these two staircase lines are disjoint and, as was mentioned above, at the last line between two nearby vertical lines there is one and only one eigenvalue point. From these two conditions it follows that the shift of the second staircase line has to be the same as of the first one. If the second line shift is less than the first line shift then we have two non-decreasing lines whose initial and final points are in different orders. But then they have to intersect which is not allowed. If the second line shift is bigger than the first line shift then it means that at the last horizontal line an eigenvalue point will be not connected to these two staircase lines. Then one can construct a staircase line starting from this point, which will go down and left. Finally such line will cross the lowest horizontal line in a certain point. But the first two constructed staircase lines were emanating from the two closest points. Therefore the descending line has to cross one of that lines, which is forbidden. These arguments show that the shift of the staircase line is independent of the choice of the initial point and it is a property of the whole eigenvalue configuration.

Let us call the vertical line from the lowest left point the base line. If the shift of the staircase line from this point equals k units ($1 \leqslant k \leqslant q - 1$) then on the last horizontal line at the right of the base line there exist $k - 1$ points which are the end points of other staircase lines emanating from $k - 1$ points at the left of the initial point. As these lines are continuous they will pass the vertical base line by certain $k - 1$ horizontal segments. If $k = 1$ there is no point between the base line and the staircase line emanating from the initial point. In this case $x_{j+1} > x_j$ for all $j = 2, \ldots, q - 1$ and there is no line where $x_{j+1} < x_j$ except, of course, $j = 1$ (cf figure 6(*b*)). Let $k > 1$. Consider the staircase line which descends from the point on the last horizontal line closest to the base line (i.e. with a shift equal to 1 unit). This line will cross the vertical base line by a certain horizontal segment belonging to the horizontal line number r_1 ($2 \leqslant r_1 \leqslant q - 1$). Going right along this horizontal line we will finally find a point which belongs to another staircase line. If $k = 2$, that line will end in

the initial point. Then the stepwise line which will be the closest to the base line (and which determines x_j) consists of two increasing staircase segments and only at one line $x_{r_1+1} < x_{r_1}$ (cf figure 7). When $k > 2$ the second staircase line will cross the base line along the horizontal line number r_2 ($2 \leqslant r_2 \leqslant r_1 - 1$). Going right along that horizontal line we will find a point from which another staircase line (different from the first two) descends. Therefore one will have $x_{r_2+1} < x_{r_2}$. And so on. In the end we find that there exist exactly $k-1$ values of j for which $x_{j+1} < x_j$. Comparing this statement with (52) we conclude that in this case there exist exactly $k-1$ Θ-functions which equal zero. All other Θ-functions will equal one. As the total number of Θ-functions is $q-2$ we find that in this case $mN \equiv -k \bmod q$ which proves the first part of the lemma, namely, that if for a configuration the shift equals k then $mN \equiv -k \bmod q$.

The inverse statement, that if $mN \equiv -k \bmod q$ then the staircase line emanating from an eigenvalue will have a shift equal to k, can be proved by the same method. Assume that $mN \equiv -k$ then from (52) it follows that $k-1$ Θ-functions have to be negative. It means that there exist $k-1$ indices $1 \leqslant j_1 < \ldots < j_{k-1} \leqslant q-1$ for which $x_{j+1} < x_j$. Let us start from the initial point and draw the staircase line which goes right and up as above. At the line number j_1 we have to jump to a point closer to the base line. After it one continues along the new increasing staircase line till it crosses the horizontal line with number j_2 where one shifts to another line and so on. The last staircase line has to have a shift equal to 1 unit. As we performed $k-1$ jumps the total shift of the staircase line from any point equals k units. Q.E.D.

When $k > q/2$ one may simplify the construction by using non-intersecting stepwise lines going up and to the left with the shift by $q-k$. It implies that properties of the cases $mN \equiv k \bmod q$ and $mN \equiv -k \bmod q$ are the same.

5. Transfer operator

The above unfolding gives not only a clear picture of mutual positions of eigenphases but also serves as the basis of the explicit calculation of the spectral statistics for the problem under consideration. The calculations are based on the following conjecture proposed in [15].

Conjecture. *For $\alpha = m/q$ the eigenvalues of the q*th *power of the original matrix (2) for all $N \not\equiv 0 \bmod q$ have universal spectral statistics independent on q and N but different for different symmetry classes of random phases Φ_k. For non-symmetric ensemble the statistics of M^q coincides with the Poisson statistics and for symmetric ensemble (4) it is described by the semi-Poisson statistics with $\beta = -1/2$ called in [15] the super-Poisson statistics.*

The main physical argument in favour of this conjecture in [15] was the fact that for rational $\alpha = m/q$ the qth power of the classical map (1) corresponds to a classically integrable map, and according to the usual wisdom [1] integrable models have to be described by the Poisson statistics. Extensive numerical calculations agree very well with this conjecture. But it seems that to prove it rigorously one has to develop new methods which are at present under investigation [19].

After unfolding, when the points from all the sectors separated by $2\pi m/q$ are taken together, they can be considered as the eigenphases of the qth power of the original matrix (with evident rescaling). Assuming the validity of the conjecture it follows that for all $N \not\equiv 0 \bmod q$ these points constitute the semi-Poisson ensemble with $\beta = 0$ for non-symmetric matrices and $\beta = -1/2$ for symmetric ones.

In particular, the probability that between two eigenvalues of M^q separated by x there exist exactly r eigenvalues is the following:

$$p_r(x) = \begin{cases} \dfrac{x^r}{r!}\mathrm{e}^{-x} & \text{for non-symmetric ensemble,} \\ \dfrac{1}{2^{(r+1)/2}\Gamma((r+1)/2)}x^{(r-1)/2}\mathrm{e}^{-x/2} & \text{for symmetric ensemble.} \end{cases} \tag{55}$$

The results of the preceding section can be reformulated such that the joint probability of the close-by levels integrated over all the possible positions of other levels is the same as the probability of non-intersecting staircase lines which start from the initial levels and which finish after q steps (where q is the denominator of α) with the shift of k units (where k is the residue of mN modulo q). According to the conjecture the distribution of unfolded points are known which permits the calculation of spectral statistics of the original matrix (2).

The usual method of computing the probability of non-intersecting paths in a Markoff process is the determinantal representation [20]. We found that for practical reasons it is more convenient to use the transfer operator method. In this method one first unfolds the spectrum as indicated in figure 7. Then one considers a vertical strip bounded by vertical lines emanating from any two nearby levels of original matrix, say θ_2 and θ_3 in figure 7 separated by the distance $x = \theta_3 - \theta_2$. Now different horizontal lines can enter and can leave the strip. When all in-coming and out-coming horizontal lines are fixed, it is obvious that the configuration inside the strip is not affected by outside points. Therefore, it is possible to integrate over all configurations of points inside the strip with prescribed ordering. Denoting the initial and final lines by indices i and j the result of integration constitutes the matrix element $T_{ji}(x)$ of the transfer matrix $T(x)$.

For rational $\alpha = m/q$ and $mN \equiv -k \bmod q$ with $1 \leqslant k \leqslant q-1$ each initial (and final) state is determined by fixing $l = k - 1$ horizontal lines:

$$1 \leqslant i_1 < i_2 < \ldots < i_l \leqslant q-2 \tag{56}$$

from the total number of lines equal $q - 2$. The number l is imposed by the shift of k units between initial and final points on the horizontal lines (cf the proof of the claim in the preceding section). It means that the dimension of the transfer operator is

$$t = C^l_{q-2} \tag{57}$$

and it is convenient to label the set of l integers obeying (56) in, e.g., lexicographical order.

For clarity, let us consider the case $\alpha = 1/5$ and $N \equiv -2 \bmod 5$ in detail ($l = 1$). As $q = 5$ there is one possible horizontal line which may go through the vertical strip (cf figure 7). Therefore the transfer matrix is 3×3 matrix labeled by the number of these lines. In figure 8 all possible configurations for this case are presented.

In general, if $i \equiv (i_1, i_2, \ldots, i_l)$ and $j \equiv (j_1, j_2, \ldots, j_l)$ are multi-indexes of an initial and a final states, the total number of points, r, inside the considered vertical strip is determined by the expression

$$r = j_1 + \sum_{s=1}^{l-1}[j_{s+1} - i_s] + q - 1 - i_l = |j| - |i| + q - 1, \tag{58}$$

where $|j| \equiv j_1 + \cdots + j_l$ and $|i| \equiv i_1 + \cdots + i_l$. The number of points r is accounted by an initial set of j_1 points as the lowest line has to exit at position j_1, a set of $q - 1 - i_l$ points as the highest entering line has to exit at the top of the diagram, and the contributions $j_{s+1} - i_s$ of points from the remaining entering and exiting lines. In general, $r_{\min} \leqslant r \leqslant r_{\max}$ with

$$r_{\min} = 2\,, \qquad r_{\max} = k(q-k). \tag{59}$$

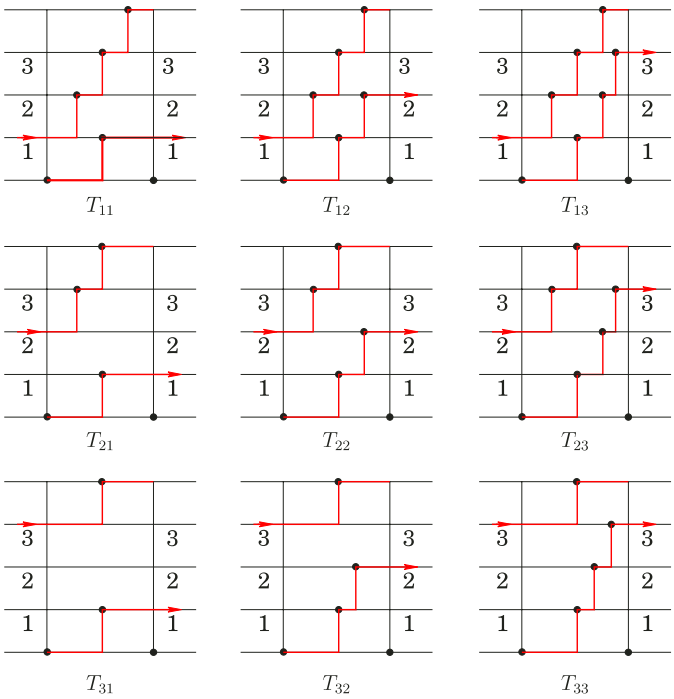

Figure 8. Structure of the transfer operator for $\alpha = 1/5$ and $N \equiv -2 \bmod 5$.

If at least one term in the square brackets in (58) is negative, the configuration is impossible and the corresponding matrix element equals zero. Otherwise, the integration over all intermediate configurations compatible with the imposed inequalities gives the value of the transfer matrix elements.

The calculation of this probability is straightforward. According to the above conjecture, the probability that between two eigenvalues of M^q separated by x there exist r ordered eigenvalues y_s such that

$$0 \leqslant y_1 \leqslant y_2 \leqslant \cdots \leqslant y_r \leqslant x \tag{60}$$

is given by (55). Therefore, the transfer matrix element $T_{ji}(x)$ is the product of two factors

$$T_{ji}(x) = n_{ji}\, p_r(x) \tag{61}$$

where r is the integer determined by (58), $p_r(x)$ is the same as in (55) and n_{ji} is the number of configurations of r points which fulfilled all inequalities comparable with the fixed initial and final states. Interchanging the initial and final states and counting horizontal lines from the top one gets that the transfer operator matrix elements obey the following symmetry:

$$T_{ji}(x) = T_{i^T j^T}(x), \tag{62}$$

where if $i = (i_1, \ldots, i_l)$, $i^T = (q - 1 - i_l, \ldots, q - 1 - i_1)$.

For example, for $\alpha = 1/5$ and $N \equiv -2 \bmod 5$ the T_{12} element includes 5 points (cf figure 8), 3 points, a, b, c belonging to the upper curve, and 2 points, A and B, belonging to the lower curve. From the mutual positions of these points it follows that the $T_{12}(x)$ matrix element equals the probability that the following inequalities are fulfilled

$$0 \leqslant a \leqslant b \leqslant c \leqslant x, \qquad 0 \leqslant A \leqslant B \leqslant x, \qquad a \leqslant A, \qquad b \leqslant B. \tag{63}$$

By inspection one finds that there exist exactly five possible ordered sequences compatible with inequalities (63), namely

$$a\ b\ c\ A\ B, \qquad a\ b\ A\ B\ c, \qquad a\ A\ b\ B\ c, \qquad a\ b\ A\ c\ B, \qquad a\ A\ b\ c\ B.$$

Therefore $T_{12}(x) = 5p_5(x)$. Following the symmetry (62) we also have $T_{23}(x) = T_{12}(x) = 5p_5(x)$.

By construction the joint probability of the eigenvalues is equal to the product of the transfer matrices over all nearby points. As we are interested in the limit of a large number of eigenvalues, the exact behaviour near the boundaries is not important and one can take simply the trace of the whole product. We are now interested in the local behaviour of the eigenvalues. To distinguish with the previous section we choose to label them x_i from now.

Finally the joint probability of an ordered sequence of $K+1$ eigenphases of the original matrix $x_1 < x_2 < \ldots < x_K < x_{K+1}$ in the interval $L = x_{K+1} - x_1$ integrated over all possible configuration of levels on other sectors takes the form

$$P_L(x_1, x_2, \ldots, x_K, x_{K+1}) = \frac{1}{Z_K(L)} \mathrm{Tr}\,[T(x_{K+1} - x_K) \cdot \ldots \cdot T(x_2 - x_1)]\, \delta(x_{K+1} - x_1 - L), \tag{64}$$

where $Z_K(L)$ is the normalization constant.

In appendix B it is demonstrated that in the limit $K \to \infty$ and $L \to \infty$ such that the mean density $L/K = 1$ the normalized nearest-neighbour distribution is determined by the formula

$$p(s) = \frac{\mathrm{e}^{-hs}}{\lambda(h)} \frac{\langle v(h) T(s) w(h) \rangle}{\langle v(h) w(h) \rangle}. \tag{65}$$

Here $\langle \cdots \rangle$ denotes scalar products as in (B.15) and (B.17).

$\lambda(\gamma)$ in (65) is the largest modulus eigenvalue of the Laplace transform of the transfer matrix

$$\hat{T}_{ij}(\gamma) = \int_0^\infty T_{ij}(x) \mathrm{e}^{-\gamma x} \mathrm{d}\, x, \tag{66}$$

and $w_j(\gamma)$ and $v_j(\gamma)$ are the corresponding right and left eigenfunctions (cf (B.6)). h in (65) denotes a special value of γ calculated from the saddle-point equation

$$\frac{\lambda'(h)}{\lambda(h)} + 1 = 0\,. \tag{67}$$

These formulae are general and can be applied for an arbitrary transfer matrix. As the x dependence of our transfer matrix $T(x)$ is given by simple formulae (61) and (55) it is easy to check that

$$w_i = \tilde{w}_i (\gamma + 1)^{|i|}, \qquad v_i = \tilde{v}_i (\gamma + 1)^{-|i|}, \qquad \lambda = \tilde{\lambda} (\gamma + 1)^{-q} \tag{68}$$

for non-symmetric matrices, and

$$w_i = \tilde{w}_i (2\gamma + 1)^{|i|/2}\,, \qquad v_i = \tilde{v}_i (2\gamma + 1)^{-|i|/2}, \qquad \lambda = \tilde{\lambda} (2\gamma + 1)^{-q/2} \tag{69}$$

for symmetric matrices. Here i denotes the multi-index $(i_1, \cdots, i_l)$, $|i| = i_1 + \ldots + i_l$ and all tilded quantities are independent of γ.

From these relations one finds that the saddle point h obeying (67) is

$$h = \begin{cases} q - 1 & \text{for non-symmetric ensemble,} \\ (q-1)/2 & \text{for symmetric ensemble.} \end{cases} \tag{70}$$

Using (59) we conclude that the nearest-neighbour distribution (65) for $\alpha = m/q$ and $mN \equiv -k \bmod q$ equals the following finite sums:

$$p(s) = \sum_{n=2}^{k(q-k)} a_n s^n \mathrm{e}^{-qs} \tag{71}$$

for non-symmetric matrices and

$$p(s) = \sum_{n=1}^{(k(q-k)-1)} a_{n/2} s^{n/2} \mathrm{e}^{-qs/2} \tag{72}$$

for symmetric ones.

The nearest-neighbour distribution for all considered cases (with $k \neq 0, \pm 1 \bmod q$) manifests level repulsion at small s

$$p(s) \sim \begin{cases} s^2 & \text{for non-symmetric ensemble,} \\ s^{1/2} & \text{for symmetric ensemble} \end{cases} \tag{73}$$

and has the exponential decrease at large s as it should be for intermediate statistics.

Other correlation functions can also be written explicitly through the same quantities [17]. In particular, the two-point correlation form factor has the following form:

$$K(\tau) = 1 + 2\mathrm{Re}\, g(2\pi \mathrm{i}\tau), \tag{74}$$

where

$$g(t) = \frac{\langle w(h) L(t+h)(1 - L(t+h))^{-1} v(h) \rangle}{\langle w(h) v(h) \rangle} \tag{75}$$

and the matrix $L(s) = \hat{T}(s)/\lambda(h)$.

One can check that for all N the level compressibility $K(0) = 1/q$ for non-symmetric matrices and $K(0) = 2/q$ for symmetric ones.

Numerically it was established [21] but not yet proved analytically that eigenvectors of the considered ensembles of random matrices have fractal properties independent of the residue $k \neq 0 \bmod q$.

6. Explicit calculations

The simplest new case corresponds to $\alpha = 1/5$ and $N \equiv \pm 2 \bmod 5$. Considering all configurations in figure 8, one gets that in this case the transfer matrix has the following form

$$T(x) = \begin{pmatrix} 3p_4(x) & 5p_5(x) & 5p_6(x) \\ 3p_3(x) & 5p_4(x) & 5p_5(x) \\ 2p_2(x) & 3p_3(x) & 3p_4(x) \end{pmatrix}. \tag{76}$$

Performing the calculations discussed in the preceding section we find that when $\alpha = 1/5$ and $N \equiv \pm 2 \bmod 5$ the nearest-neighbour distribution for non-symmetric matrices is

$$p(s) = (a_2 s^2 + a_3 s^3 + a_4 s^4 + a_5 s^5 + a_6 s^6) e^{-5s}, \tag{77}$$

where coefficients a_n are the following: $a_2 = 625/2 - 275\sqrt{5}/2 \approx 5.041$, $a_3 = 3125/2 - 1375\sqrt{5}/2 \approx 25.203$, $a_4 = 71875/48 + 33125\sqrt{5}/48 \approx 45.724$, $a_5 = -15625/3 + 9375\sqrt{5}/4 \approx 32.451$, $a_6 = 1015625/288 - 453125\sqrt{5}/288 \approx 8.357$.

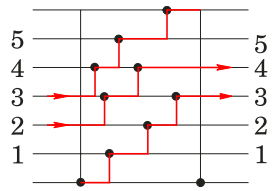

Figure 9. One of the transfer matrix elements for $\alpha = 1/7$ and $N \equiv -3 \bmod 7$.

In a similar manner one finds that for symmetric matrices under the same conditions $p(s)$ is given by the following expression:

$$p(s) = (a_{1/2}s^{1/2} + a_1 s + a_{3/2}s^{3/2} + a_2 s^2 + a_{5/2}s^{5/2})e^{-5s} \tag{78}$$

with $a_{1/2} \approx 0.3597$, $a_1 \approx 1.5122$, $a_{3/2} \approx 2.6105$, $a_2 \approx 1.9471$, $a_{5/2} \approx 0.5725$.

For $\alpha = 1/7$ and $N \equiv \pm 2 \bmod 7$ the transfer operator is represented by the 5×5 matrix:

$$T(x) = \begin{pmatrix} 5p_6(x) & 14p_7(x) & 28p_8(x) & 42p_9(x) & 42p_{10}(x) \\ 5p_5(x) & 14p_6(x) & 28p_7(x) & 42p_8(x) & 42p_9(x) \\ 4p_4(x) & 10p_5(x) & 19p_6(x) & 28p_7(x) & 28p_8(x) \\ 3p_3(x) & 6p_4(x) & 10p_5(x) & 14p_6(x) & 14p_7(x) \\ 2p_2(x) & 3p_3(x) & 4p_4(x) & 5p_5(x) & 5p_6(x) \end{pmatrix}. \tag{79}$$

Computing its largest eigenvalue and using (65) one finds that the nearest-neighbour distribution in this case for non-symmetric matrices has the form

$$p(s) = (a_2 s^2 + a_3 s^3 + a_4 s^4 + a_5 s^5 + a_6 s^6 + a_7 s^7 + a_8 s^8 + a_9 s^9 + a_{10} s^{10})\mathrm{e}^{-7s}, \tag{80}$$

where coefficients a_n are $a_2 \simeq 3.4998$, $a_3 \simeq 24.4986$, $a_4 \simeq 82.4309$, $a_5 \simeq 176.8723$, $a_6 \simeq 251.6396$, $a_7 \simeq 229.5488$, $a_8 \simeq 130.8981$, $a_9 \simeq 43.7932$, $a_{10} \simeq 6.8214$.

For symmetric matrices for the same α and N

$$p(s) = (a_{1/2}\sqrt{s} + a_1 s + a_{3/2}s^{3/2} + a_2 s^2 + a_{5/2}s^{5/2} + a_3 s^3 + a_{7/2}s^{7/2} + a_4 s^4 + a_{9/2}s^{9/2})\mathrm{e}^{-7s/2} \tag{81}$$

with $a_{1/2} \simeq 0.1508$, $a_1 \simeq 0.7500$, $a_{3/2} \simeq 2.0293$, $a_2 \simeq 3.8675$, $a_{5/2} \simeq 5.3099$, $a_3 \simeq 5.0193$, $a_{7/2} \simeq 3.1567$, $a_4 \simeq 1.2312$, $a_{9/2} \simeq 0.2350$.

For $\alpha = 1/7$ and $N \equiv \pm 3 \bmod 7$ there exist two possible entering lines and two leaving lines (cf figure 9) The dimension of the transfer matrix in this case is $C_5^2 = 10$. Its explicit

form is the following:

$$T(x) = \begin{pmatrix} 10p_6 & 35p_7 & 70p_8 & 84p_9 & 56p_8 & 168p_9 & 252p_{10} & 210p_{10} & 462p_{11} & 462p_{12} \\ 10p_5 & 35p_6 & 70p_7 & 84p_8 & 56p_7 & 168p_8 & 252p_9 & 210p_9 & 462p_{10} & 462p_{11} \\ 6p_4 & 20p_5 & 40p_6 & 49p_7 & 30p_6 & 91p_7 & 140p_8 & 112p_8 & 252p_9 & 252p_{10} \\ 3p_3 & 8p_4 & 15p_5 & 19p_6 & 10p_5 & 30p_6 & 49p_7 & 35p_7 & 84p_8 & 84p_9 \\ 4p_4 & 15p_5 & 30p_6 & 35p_7 & 26p_6 & 77p_7 & 112p_8 & 98p_8 & 210p_9 & 210p_{10} \\ 3p_3 & 12p_4 & 25p_5 & 30p_6 & 20p_5 & 61p_6 & 91p_7 & 77p_7 & 168p_8 & 168p_9 \\ 2p_2 & 6p_3 & 12p_4 & 15p_5 & 8p_4 & 25p_5 & 40p_6 & 30p_6 & 70p_7 & 70p_8 \\ 0 & 3p_3 & 8p_4 & 10p_5 & 6p_4 & 20p_5 & 30p_6 & 26p_6 & 56p_7 & 56p_8 \\ 0 & 2p_2 & 6p_3 & 8p_4 & 3p_3 & 12p_4 & 20p_5 & 15p_5 & 35p_6 & 35p_7 \\ 0 & 0 & 2p_2 & 3p_3 & 0 & 3p_3 & 6p_4 & 4p_4 & 10p_5 & 10p_6 \end{pmatrix}. \tag{82}$$

Finally one obtains that for $\alpha = 1/7$ and $N \equiv \pm 3 \bmod 7$ the nearest-neighbour distribution for non-symmetric ensemble is

$$p(s) = (a_2 s^2 + a_3 s^3 + a_4 s^4 + a_5 s^5 + a_6 s^6 + a_7 s^7 + a_8 s^8 + a_9 s^9 + a_{10} s^{10} + a_{11} s^{11} + a_{12} s^{12}) \mathrm{e}^{-7s} \tag{83}$$

where $a_2 \simeq 4.056$, $a_3 \simeq 28.3898$, $a_4 \simeq 91.6591$, $a_5 \simeq 177.9134$, $a_6 \simeq 227.8782$, $a_7 \simeq 200.0096$, $a_8 \simeq 121.6091$, $a_9 \simeq 50.5880$, $a_{10} \simeq 13.778$, $a_{11} \simeq 2.2159$, $a_{12} \simeq 0.1596$.

For symmetric matrices under the same conditions

$$p(s) = (a_{1/2}\sqrt{s} + a_1 s + a_{3/2} s^{3/2} + a_2 s^2 + a_{5/2} s^{5/2} + a_3 s^3 + a_{7/2} s^{7/2} + a_4 s^4 + a_{9/2} s^{9/2} + a_5 s^5 + a_{11/2} s^{11/2}) \mathrm{e}^{-7s/2} \tag{84}$$

with $a_{1/2} \simeq 0.1747$, $a_1 \simeq 0.8691$, $a_{3/2} \simeq 2.2565$, $a_2 \simeq 3.8902$, $a_{5/2} \simeq 4.8085$, $a_3 \simeq 4.3734$, $a_{7/2} \simeq 2.9327$, $a_4 \simeq 1.4222$, $a_{9/2} \simeq 0.4747$, $a_5 \simeq 0.0979$, $a_{11/2} \simeq 0.0094$.

In figures 10 and 11 the calculated nearest neighbour distributions are plotted for $\alpha = 1/5$ and $\alpha = 1/7$ with all possible residues of $N \not\equiv 0$ modulo $1/\alpha$. As expected, the case $N \equiv \pm 1 \bmod 1/\alpha$ differs considerably from other cases. When the residue, k, increases the nearest-neighbour distribution more and more resembles to the nearest-neighbour distribution of the standard Gaussian ensembles of random matrices. For example, for $\alpha = 1/7$ the results with $N \equiv \pm 2$ and $N \equiv \pm 3$ are difficult to distinguish from the Wigner surmise (8) for GUE (for non-symmetric matrices) and for GOE (for symmetric ones).

To compare these formulae with the results of the numerical simulations it is more precise to use the integrated nearest-neighbour distribution (16). In figures 12 and 13 such comparison is performed for all the cases considered. The agreement is quite good and the differences are of the same order as in figure 2.

7. Summary

A unitary random matrix ensemble

$$M_{kp} = \mathrm{e}^{\mathrm{i}\Phi_k} \frac{(1 - \mathrm{e}^{2\pi \mathrm{i}\alpha N})}{N(1 - \mathrm{e}^{2\pi \mathrm{i}(k-p+\alpha N)/N})} \tag{85}$$

corresponding to a quantization of a simple pseudo-integrable map (1) is considered in detail. These matrices are characterized by a rational parameter $\alpha = m/q$, the matrix dimension N and symmetry properties of random phases Φ_k (4). To get a well-defined limit of the spectral statistics of these ensembles for large N it is necessary to consider increasing sequences of N such that mN has a fixed residue modulo the denominator of α:

$$mN \equiv -k \bmod q \tag{86}$$

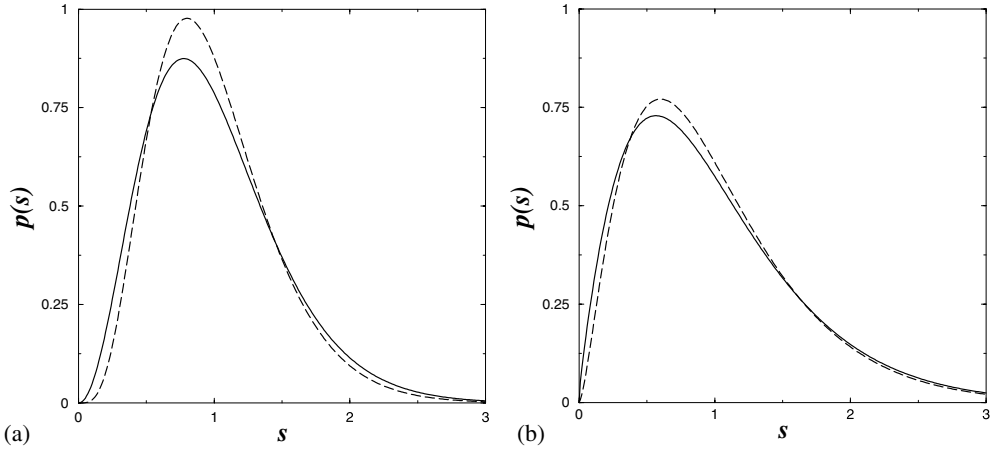

Figure 10. Nearest-neighbour distribution for $\alpha = 1/5$ for (a) the non-symmetric ensemble and (b) the symmetric one. Dashed lines correspond to $N \equiv \pm 1 \bmod 5$ given by (13) with $\beta = 4$ in (a) and $\beta = 3/2$ in (b). Solid lines indicate the results for $N \equiv \pm 2 \bmod 5$ given by (77) in (a) and by (78) in (b).

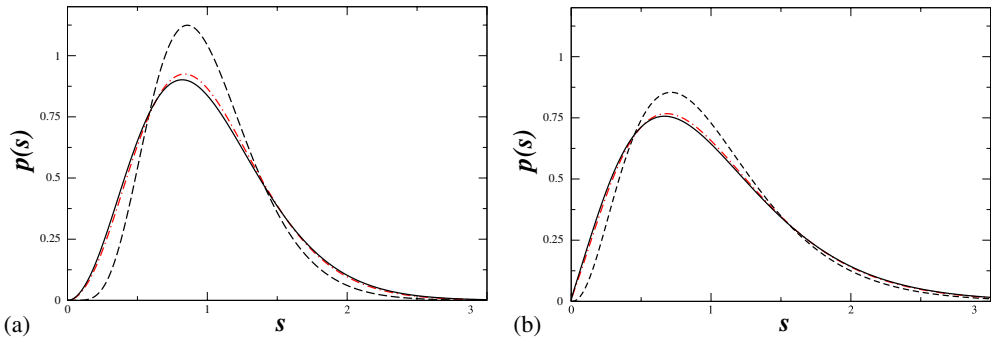

Figure 11. The same as in figure 10 but for $\alpha = 1/7$. Dashed black lines correspond to $N \equiv \pm 1 \bmod 7$ given by (13) with $\beta = 6$ in non-symmetric matrices and $\beta = 3/2$ for symmetric matrices. The red dotted–dashed lines indicate the results for $N \equiv \pm 2 \bmod 7$ given by (80) in (a) and by (81) in (b). Solid black lines represent the results for $N \equiv \pm 3 \bmod 7$ determined by (83) in (a) and by (84) in (b).

with the residue $k = 0, 1, \ldots, q-1$. For $k = 0$ all eigenvalues of the main matrix can be found analytically as in [14]. For all other residues the spectral statistics of the considered ensembles is non-trivial and differs considerably from standard random matrix ensembles. The cases $k = 1$ and $k = q - 1$ have been investigated in [15] where it was shown that for these k the nearest-neighbour distribution has the following form:

$$p(s) \sim \begin{cases} s^{q-1}\mathrm{e}^{-qs} & \text{for non-symmetric ensemble,} \\ s^{q/2-1}\mathrm{e}^{-qs/2} & \text{for symmetric ensemble.} \end{cases} \tag{87}$$

In this paper a kind of transfer operator method is developed to calculate the spectral statistics of the same matrix for all values of k. It is demonstrated that the nearest-neighbour distribution equals the product of a finite polynomial in s for non-symmetric matrices and in $\sqrt{s}$ for

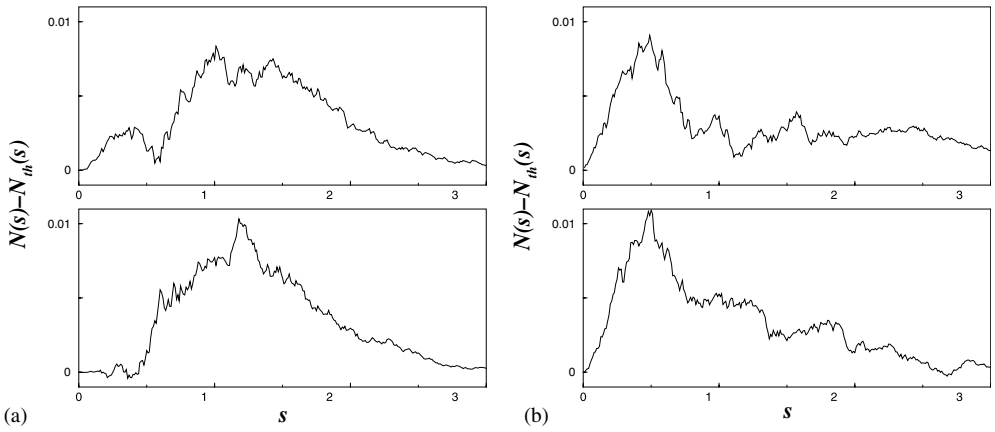

Figure 12. Difference between the integrated nearest-neighbour distribution and the corresponding theoretical prediction for $\alpha = 1/5$: (*a*) for non-symmetric ensembles, (*b*) for symmetric matrices. In each graph pictures differ by the matrix dimensions. From bottom to top $N = 801$ ($N \equiv 1 \bmod 5$) and 802 ($N \equiv 2 \bmod 5$).

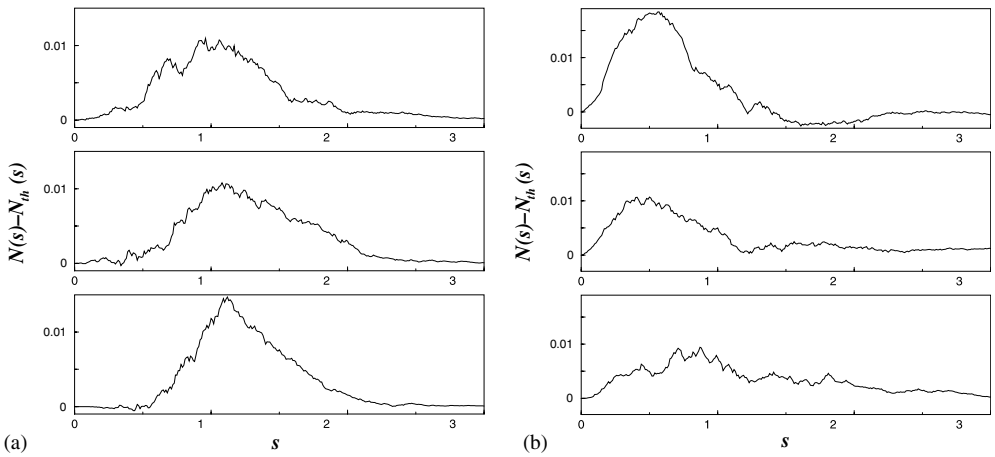

Figure 13. The same as in figure 12 but for $\alpha = 1/7$. From bottom to top $N = 799$ ($N \equiv 1 \bmod 7$), 800 ($N \equiv 2 \bmod 7$) and 801 ($N \equiv 3 \bmod 7$).

symmetric matrices times the same exponential factor as in (87)

$$p(s) = \begin{cases} \displaystyle\sum_{n=2}^{k(q-k)} a_n s^n \mathrm{e}^{-qs} & \text{for non-symmetric ensemble,} \\ \displaystyle\sum_{n=1}^{(k(q-k)-1)} a_{n/2} s^{n/2} \mathrm{e}^{-qs/2} & \text{for symmetric ensemble.} \end{cases} \tag{88}$$

Statistical properties of sequences with residue k and $q - k$ are the same. The values of coefficients a_n can be calculated by finding the largest eigenvalue and the corresponding left and right eigenvectors of the transfer matrix.

For $\alpha = 1/5$ and $\alpha = 1/7$ and all possible residues the explicit form of these coefficients have been calculated. Numerical simulations in these cases are in good agreement with the obtained formulae. Other correlation functions can also be expressed from the same quantities.

It appears that the considered ensembles of random matrices permit different generalizations which will be discussed elsewhere [19].

Acknowledgments

It is a pleasure to thank O Bohigas and O Giraud for helpful discussions and J Marklof for a careful reading of the manuscript. RD wishes to acknowledge financial support from the 'Programme Lavoisier' of the French Ministère des Affaires étrangères et européennes and EPSRC.

Appendix A. Algebraic relations

The purpose of the appendix is to give the proofs of certain formulae used in the text.

Let for all $n = 1, \ldots, N$

$$\sum_{m=1}^{N} \frac{b_m}{x_m - y_n} = 1. \tag{A.1}$$

Solutions b_m of these equations can be expressed in terms of Cauchy determinants and

$$b_m = \frac{\prod_n (x_m - y_n)}{\prod_{s \neq m} (x_m - x_s)}. \tag{A.2}$$

A simple way to check it is to consider the function

$$f_n(x) = \frac{\prod_{r \neq n} (x - y_r)}{\prod_s (x - x_s)} = \frac{\prod_r (x - y_r)}{(x - y_n) \prod_s (x - x_s)}. \tag{A.3}$$

Asymptotically $f_n(x) \to 1/x$ so the integral over a big contour encircling all poles equals $2\pi \mathrm{i}$. Rewriting this integral as the sum over the poles gives

$$1 = \sum_m \frac{\prod_r (x_m - y_r)}{(x_m - y_n) \prod_{s \neq m} (x_m - x_s)} \tag{A.4}$$

which proves (A.2).

Denote

$$g(x) = \frac{\prod_n (x - \Lambda_n \mathrm{e}^{2\pi \mathrm{i}\alpha})}{x \prod_k (x - \Lambda_k)}. \tag{A.5}$$

This function decreases as $1/x$ for large x and has poles at $x = 0$ and $x = \Lambda_k$. Integrating it over a contour encircling all poles one gets

$$1 = \mathrm{e}^{2\pi \mathrm{i} N \alpha} + \sum_{m=1}^{N} \frac{\prod_n (\Lambda_m - \Lambda_n \mathrm{e}^{2\pi \mathrm{i}\alpha})}{\Lambda_m \prod_{k \neq m} (\Lambda_m - \Lambda_k)} \tag{A.6}$$

from which it follows that $|B_m|^2$ defined by (41) obeys automatically the normalization condition (33).

Appendix B. Transfer operator calculations

The purpose of this appendix is to derive the nearest-neighbour distribution of eigenvalues when their joint probability has the form of the product of transfer matrices as in (64). The material is not new (see e.g. [17] and references therein) and presented here for convenience.

Introducing the differences between consecutive eigenvalues

$$\xi_j = x_{j+1} - x_j \tag{B.1}$$

the probability (64) can be rewritten as follows:

$$P_L(\xi_1, \ldots, \xi_K) = \frac{1}{Z_K(L)} \mathrm{Tr}\left[T(\xi_K) \cdot \ldots \cdot T(\xi_2) \cdot T(\xi_1))\right] \delta(\xi_1 + \xi_2 + \cdots + \xi_K - L)\,. \tag{B.2}$$

The normalization constant $Z_K(L)$ is determined from

$$Z_K(L) = \int_0^\infty \mathrm{d}\xi_K \ldots \int_0^\infty \mathrm{d}\xi_1 P_L(\xi_1, \ldots, \xi_K). \tag{B.3}$$

Due to the special structure of $P_L(\xi_1, \ldots, \xi_K)$ in (B.2) these integrals are of convolution type and can be calculated by the Laplace transform. One gets

$$\hat{Z}_K(\gamma) \equiv \int_0^\infty Z_K(L)\mathrm{e}^{-\gamma L}\mathrm{d}L = \mathrm{Tr}\left[\hat{T}(\gamma)\right]^K, \tag{B.4}$$

where matrix $\hat{T}(\gamma) \equiv \hat{T}_{ij}(\gamma)$ is the Laplace transform of initial transfer matrix $T_{ij}(x)$

$$\hat{T}_{ij}(\gamma) = \int_0^\infty T_{ij}(x)\mathrm{e}^{-\gamma x}\mathrm{d}\,x. \tag{B.5}$$

As $\mathrm{Tr}\big[\hat{T}(\gamma)\big]^K = \sum_j \lambda_j^K$ where λ_j are eigenvalues of matrix $\hat{T}(\gamma)$, in the limit $K \to \infty$ the dominant contribution comes from an eigenvalue with the largest modulus. Denote such eigenvalue by $\lambda(\gamma)$ and the corresponding right and left eigenfunctions by $w_j(\gamma)$ and $v_j(\gamma)$, respectively:

$$\sum_j \hat{T}_{ij}(\gamma) w_j(\gamma) = \lambda(\gamma) w_i(\gamma), \qquad \sum_i v_i(\gamma)\hat{T}_{ij}(\gamma) = \lambda(\gamma) v_j(\gamma). \tag{B.6}$$

As stated, when $K \to \infty$

$$\hat{Z}_K(\gamma) \to (\lambda(\gamma))^K. \tag{B.7}$$

The normalization constant is obtained from this quantity by the inverse Laplace transform

$$Z_K(L) = \frac{1}{2\pi \mathrm{i}} \int_{c-\mathrm{i}\infty}^{c+\mathrm{i}\infty} (\lambda(\gamma))^K \mathrm{e}^{\gamma L}\mathrm{d}\gamma, \tag{B.8}$$

where c is greater than all singularities of $\lambda(\gamma)$.

We are interested in the limit $K \to \infty$ and $L \to \infty$ but when the mean level density L/K is kept constant, which from now we normalize to 1. In this case the main contribution to the above integral comes from a vicinity of a saddle point $\gamma = h$ determined from the saddle-point condition

$$\frac{\lambda'(h)}{\lambda(h)} + 1 = 0. \tag{B.9}$$

Shifting the integration contour that it passes through the saddle point gives

$$Z_K(L) \sim (\lambda(h))^K \mathrm{e}^{hL}. \tag{B.10}$$

The pre-factor is irrelevant for our purpose.

The nearest-neighbour distribution is determined by the integration of (B.2) over all but one variables

$$p_K(s;L) = \frac{1}{Z_N(L)} R_K(s;L), \tag{B.11}$$

where

$$R_K(s;L) = \int_0^\infty \mathrm{d}\xi_K \ldots \int_0^\infty \mathrm{d}\xi_2 \mathrm{Tr}\left[T(\xi_K)\cdot\ldots\cdot T(\xi_2)\cdot T(s))\right]\delta(s+\xi_2+\cdots+\xi_K - L). \tag{B.12}$$

Performing the Laplace transform of the both parts of this expression we obtain in the same way as above that

$$\hat{R}_K(s;\gamma) \equiv \int_0^\infty p_K(s;L)\mathrm{e}^{-\gamma L}\mathrm{d}L = \mathrm{Tr}\left[\left(\hat{T}(\gamma)\right)^{K-1} T(s)\right]. \tag{B.13}$$

Matrix $\left(\hat{T}(\gamma)\right)^{K-1}$ has the same eigenfunctions as matrix $\hat{T}(\gamma)$ and its eigenvalues equal $(K-1)$th power of the ones of $\hat{T}(\gamma)$. Therefore in the limit $K\to\infty$

$$\left[\left(\hat{T}(\gamma)\right)^{K-1}\right]_{ij} \to (\lambda(\gamma))^{K-1}\frac{w_i(\gamma)v_j(\gamma)}{\langle v(\gamma)w(\gamma)\rangle}. \tag{B.14}$$

Here

$$\langle v(\gamma)w(\gamma)\rangle = \sum_t v_t(\gamma)w_t(\gamma) \tag{B.15}$$

is the scalar product of left and right eigenfunctions of $\hat{T}(\gamma)$ introduced to normalize these eigenfunctions.

$R_K(s;L)$ is obtained from its Laplace transform by standard formula (B.8). As above, the dominant contribution will be given by the same saddle point as in (67). Performing simple calculations one finds that normalized nearest-neighbour distribution when $L/K = 1$ and $K\to\infty$ is given by the following general formula

$$p(s) = \frac{\mathrm{e}^{-hs}}{\lambda(h)}\frac{\langle v(h)T(s)w(h)\rangle}{\langle v(h)w(h)\rangle}, \tag{B.16}$$

where

$$\langle v(h)T(s)w(h)\rangle = \sum_{ij} v_i(h)T_{ij}(s)w_j(h)\ . \tag{B.17}$$

Due to (67) $p(s)$ in the above expression obeys the standard normalization conditions

$$\int_0^\infty p(s)\,\mathrm{d}s = 1, \qquad \int_0^\infty sp(s)\,\mathrm{d}s = 1. \tag{B.18}$$

References

[1] Berry M and Tabor M 1977 Level clustering in the regular spectrum *Proc. R. Soc. Lond.* A **356** 375

[2] Bohigas O, Giannoni M-J and Schmit C 1984 Characterization of chaotic quantum spectra and universality of level fluctuation laws *Phys. Rev. Lett.* **52** 1

[3] Bogomolny E, Georgeot B, Giannoni M-J and Schmit C 1997 Arithmetical chaos *Phys. Rep.* **291** 220

[4] Richens P J and Berry M V 1981 Pseudointegrable systems in classical and quantum mechanics *Physica D: Nonlinear Phenom.* **2** 495

[5] Zemlyakov A N and Katok A B 1975 Topological transitivity in billiards in polygons *Math. Notes* **18** 760

[6] Bogomolny E, Gerland U and Schmit C 1999 Models of intermediate spectral statistics *Phys. Rev.* E **59** R1315

[7] Shklovskii B I, Shapiro B, Sears B R, Lambrianides P and Shore H B 1993 Statistics of spectra of disordered systems near the metal–insulator transition *Phys. Rev.* B **47** 11487

[8] Evers F and Mirlin A D 2008 Anderson transitions *Rev. Mod. Phys.* **80** 1355
[9] Bogomolny E, Giraud O and Schmit C 2001 Periodic orbits contribution to the 2-point correlation form factor for pseudo-integrable systems *Commun. Math. Phys.* **222** 327
[10] Sommerfeld A 1954 *Optics* (New York: Academic)
[11] Bogomolny E and Schmit C 2004 Structure of wave functions of pseudointegrable billiards *Phys. Rev. Lett.* **92** 244102
[12] Bogomolny E, Dietz B, Friedrich T, Miski-Oglu M and Richter A 2006 *Phys. Rev. Lett.* **97** 254102
[13] Giraud O, Marklof J and O'Keefe S 2004 Intermediate statistics in quantum maps *J. Phys. A: Math. Gen.* **37** L303
[14] Marklof J and Rudnick Z 2000 Quantum unique ergodicity for parabolic map *Geom. Funct. Anal.* **10** 1554
[15] Bogomolny E and Schmit C 2004 Spectral statistics of a quantum interval-exchange map *Phys. Rev. Lett.* **93** 254102
[16] Mehta M L 2004 *Random Matrices* (New York: Academic)
[17] Bogomolny E, Gerland U and Schmit C 2001 Short range plasma models for intermediate spectral statistics *Eur. Phys. J.* B **19** 121
[18] Albeverio S, Gesztesy F, Hoegh-Krohn R and Holgen H 1988 *Solvable Models in Quantum Mechanics* (New York: Springer)
[19] Bogomolny E, Giraud O and Schmit C 2009 Random matrix ensembles associated with Lax matrices *Phys. Rev. Lett.* submitted arXiv:nlin.0904.4898
[20] Karlin S and McGregor J 1959 Coincidence probabilities *Pacific J. Math.* **9** 1141
[21] Martin M, Giraud O and Georgeot B 2008 Multifractality and intermediate statistics in quantum maps *Phys. Rev.* E **77** 035201